THE ASTROPHYSICAL JOURNAL SUPPLEMENT SERIES, 120:327–334, 1999 February

ELECTRON-ION RECOMBINATION OF Fe V

SULTANA N. NAHAR AND MANUEL A. BAUTISTA[1]
Department of Astronomy, The Ohio State University, Columbus, OH 43210
Received 1998 July 2; accepted 1998 September 1

ABSTRACT

Ionization balance in the low-ionization stages of iron is important in a variety of astrophysical plasmas. Accurate recombination rates are needed but are difficult to compute in a detailed quantum mechanical treatment. The main difficulty lies in the complexity of strong electron-electron correlation arising due to the open 3*d* shell. We present the total electron-ion recombination rate coefficients for the process, e + Fe VI → Fe V, obtained in an ab initio manner. Large-scale computations are carried out in the close coupling (CC) approximation using the *R*-matrix method employing a unified treatment that considers the infinite number of states of the recombined ion and incorporates both the radiative recombiantion (RR) and the dielectronic recombination (DR) processes in a self-consistent manner. It involves calculations of detailed photoionization cross sections, $\sigma_{\rm PI}$, with autoionizing resonances of a large number of bound states with $n \le n_{\rm max}$, such as 1054 bound states for the present case of Fe V. The number also equals the total number of state-specific recombination rates obtained for the ion. The high-*n* states are treated through the DR theory by Bell & Seaton. The same wavefunction expansion is employed in all photoionization/recombination calculations, thereby ensuring self-consistency. Rates are presented at a wide range of temperature for all practical applications. Present rates for total recombination differ considerably from currently used values obtained using simpler approximations. Application of the new recombination rate coefficients and photoionization cross sections for the ionization structure of iron in planetary nebulae show that under typical conditions the relative fractions of Fe V and Fe VI change by nearly a factor of 2.

Subject headings: atomic data — atomic processes — planetary nebulae: general

1. INTRODUCTION

Iron ions in low-ionization stages are prominent in various astronomical sources such as diffuse and planetary nebulae (Osterbrock 1989; Peimbert 1989). Observations of Fe V spectra have also been made in young, hot DA white dwarf atmospheres by the *International Ultraviolet Explorer* (*IUE*) and the *Extreme Ultraviolet Explorer* (*EUVE*; Koester 1996; Vennes 1996; Barstow et al. 1996). A large amount of atomic data is needed in order to fully model the iron ions, especially the non-LTE spectral synthesis models. With this aim we are carrying out extensive calculations for excitation, photoionization, and recombination of iron ions (Bautista & Pradhan 1998 and references therein).

The aim of the present work (and similar previous works) is to calculate total recombination rate coefficients, $\alpha_R(T)$, taking into account two important factors: (1) the recombination rates should be consistent with the photoionization cross sections for a precise treatment of ionization balance; (2) recombination via the nonresonant background (radiative recombination, hereafter RR) and the resonances (dielectronic recombination, hereafter DR) should be included in a unified manner (e.g., Nahar, Bautista, & Pradhan 1997, 1998; Nahar 1996, 1997). Owing to the difficulties in representing many-electron ions by accurate wavefunctions and complexities of strong electron-electron correlation, no such studies of recombination processes were carried out in the past. However, significant advances have been made under the Opacity Project (OP; Seaton 1987; Berrington et al. 1987) and the Iron Project (IP; Hummer et al. 1993) in systematic studies of radiative and collisional processes in an ab initio manner in the close coupling (CC) approximation employing the *R*-matrix method. The close coupling *R*-matrix method has been extended recently to calculations of total recombination cross sections using the unified treatment (Nahar & Pradhan 1994, 1995), which incorporates the radiative and dielectronic recombinations processes in an ab inito manner. The treatment is being implemented at present to large-scale computations for total $\alpha_R(T)$ of iron ions. In this report we present these for e + Fe VI → Fe V at a wide range of temperatures and compare with currently available recombination rates for Fe V (Woods, Shull, & Sarazin 1981; Hahn 1989) obtained with separate (and relatively simple) treatments for RR using the central field and hydrogenic approximations and for DR using the Burgess General formula. The state-specific recombination rates for a large number of bound states of Fe V are also presented for the first time.

2. THEORETICAL SUMMARY AND COMPUTATIONS

Photoionization and recombination are considered in a self-consistent manner within the same theoretical formulation. The details of the close coupling (CC) calculations using the unified treatment for electron-ion recombination are described in Nahar & Pradhan (1994, 1995; Nahar 1996). The treatment considers the infinite number of recombined states. The states are divided into two groups: (A) low-*n* bound states, ranging from the ground state to excited states with $n \le n_{\rm max}$, and (B) high-*n* states, $n_{\rm max} < n \le \infty$. Typical choice for $n_{\rm max}$ is 10 (11 in a few cases). Group A states are treated via photorecombination using detailed balance with photoionization in the energy range where both the background and resonant recombinations are important. The recombination rates are obtained from

[1] Laboratory for High Energy Astrophysics, Code 662, NASA Goddard Space Flight Center, Greenbelt, MD 20771.

the photoionization cross sections of a large number of bound states. As these cross sections include the detailed structures of autoionizing resonances, the sum of individual rates of the bound states corresponds to inclusion of both the RR and the DR in a unified manner. Group B states are dense and belong to small energy regions below target thresholds where dielectronic recombination dominates. These states are treated through the DR theory by Bell & Seaton (1985; Nahar & Pradhan 1994).

Extensive large-scale computations are carried out for the atomic data of the ion. Some computational details are described. In the CC approximation the target (recombining ion) is represented by an N-electron system, and the recombined ion by an $(N + 1)$ electron system. The total wavefunction expansion, $\Psi(E)$, of the $(N + 1)$ electron system for any symmetry $SL\pi$ is represented in terms of the target wavefunctions as

$$\Psi(E) = A \sum_i \chi_i \theta_i + \sum_j c_j \Phi_j , \quad (1)$$

where χ_i is the target wavefunction in a specific state $S_i L_i \pi_i$ and θ_i is the wavefunction for the $(N + 1)$th electron in a channel labeled as $S_i L_i \pi_i k_i^2 \ell_i (SL\pi)$; k_i^2 being its kinetic energy. Φ_j's are the bound channel functions of the $(N + 1)$-electron system that account for short range correlation and the orthogonality between the continuum and the bound orbitals. For the recombination calculations of Fe v an eigenfunction expansion of 34 states of Fe vi, which includes most of the dominant terms from the ground $3d^3$, and excited $3d^2 4s$, and $3d^2 4p$ configurations is employed (Bautista 1996). The target wavefunctions were obtained using atomic structure code SUPERSTRUCTURE (Eissner et al. 1974; Eissner 1991). Although the calculated energies of Fe vi agree quite well with the observed energies, as discussed in Bautista (1996), observed energies are used in the present calculations for more accurate positions of the resonances. Both the target states and the observed energies used are given in Table 1.

2.1. *Low-n States: Photoionization Cross Sections*

In the unified treatment the partial photoionization cross sections leaving the core in the ground state are calculated for all group A low-n bound states. The recombination cross sections, $\sigma_{\rm RC}$, are then obtained from the photoionization cross sections, $\sigma_{\rm PI}$, through principle of detailed balance as

$$\sigma_{\rm RC} = \frac{g_i}{g_f} \frac{h^2 v^2}{m^2 v^2 c^2} \sigma_{\rm PI} , \quad (2)$$

where g_i and g_f are the statistical weight factors of the initial and final states, respectively, v is the velocity of the photoelectron, and ν is the photon frequency. The recombination rate coefficient at a given temperature is obtained by averaging $\sigma_{\rm RC}(T)$ over the Maxwellian distribution of electrons, $f(v)$, as

$$\alpha_R(T) = \int_0^\infty v f(v) \sigma_{\rm RC} \, dv$$
$$= \frac{g_i}{g_j} \frac{2}{kT\sqrt{2\pi m^3 kc^2 T}} \int_0^\infty E^2 \sigma_{\rm PI}(\epsilon) e^{-\epsilon/kT} d\epsilon , \quad (3)$$

where $E = \hbar\omega = \epsilon + I_p$, ϵ is the photoelectron energy, and I_p is the ionization potential.

We obtain 1054 bound states of Fe v in group A, of which 266 are quintets and 788 triplets, that couple to the core ground state, $3d^3(^4F)$ of Fe vi and calculate $\sigma_{\rm PI}$ with autoionizing resonances for all these states. Computations are carried out in a manner described in Bautista (1996) using the R-matrix codes from the Opacity Project (Seaton 1987; Berrington et al. 1987) extended for the Iron Project (Hummer et al. 1993), and a modified version of the program STGBF (Nahar & Pradhan 1995). Values of $\sigma_{\rm PI}$ in the present work are calculated new since only the *total* photoionization cross sections were obtained in Bautista (1996), while *partial* photoionization cross sections leaving the core ion in the ground state are needed for the recombination rates. The recombination rate coefficients of individual bound states are obtained by averaging over $\sigma_{\rm RC}(T)$ using the code RECOMB (Nahar 1996). The low-n contributions to the total recombiation rate coefficients are then obtained by summing the individaul contributions of these bound states. Some details of computations of $\sigma_{\rm RC}$ for the entire energy range of the photoelectron up to ∞ is given in Nahar & Pradhan (1994).

The percentage contributions of individual bound states to total α_R and the order of contributing states are not the same at all temperatures but vary due to resonance structures and enhancement in the background cross sections. While the ground state is not necessarily the most dominant state, equivalent electron states often are dominant contrib-

TABLE 1

THE LS TERMS AND ENERGIES, E_t (IN ryd), OF Fe VI IN THE EIGENFUNCTION EXPANSION OF Fe V

Number	Term	E_t	Number	Term	E_t	Number	Term	E_t
1	$3d^3(^4F)$	0.0	13	$3d^2 4s(^2P)$	2.6175	25	$3d^2 4p(^2F^o)$	3.2628
2	$3d^3(^4P)$	0.1647	14	$3d^2 4s(^2G)$	2.6532	26	$3d^2 4p(y^4D^o)$	3.2792
3	$3d^3(^2G)$	0.1808	15	$3d^2 4s(^2S)$	3.0659	27	$3d^2 4p(^2D^o)$	3.2910
4	$3d^3(^2P)$	0.2291	16	$3d^2 4p(^4G^o)$	3.0933	28	$3d^2 4p(^4P^o)$	3.3143
5	$3d^3(^2D)$	0.2495	17	$3d^2 4p(^4F^o)$	3.0993	29	$3d^2 4p(^2G^o)$	3.3172
6	$3d^3(^2H)$	0.2535	18	$3d^2 4p(^2F^o)$	3.1165	30	$3d^2 4p(^2D^o)$	3.3662
7	$3d^3(^2F)$	0.4121	19	$3d^2 4p(z^4D^o)$	3.1283	31	$3d^2 4p(^2H^o)$	3.3882
8	$3d^3(^2D)$	0.6441	20	$3d^2 4p(^2D^o)$	3.1370	32	$3d^2 4p(^2P^o)$	3.4004
9	$3d^2 4s(^4F)$	2.3873	21	$3d^2 4p(^2G^o)$	3.1747	33	$3d^2 4p(^2F^o)$	3.4379
10	$3d^2 4s(^2F)$	2.4500	22	$3d^2 4p(^2S^o)$	3.1953	34	$3d^2 4p(^2P^o)$	3.7225
11	$3d^2 4s(^2D)$	2.5503	23	$3d^2 4p(^4S^o)$	3.2304			
12	$3d^2 4s(^4P)$	2.5628	24	$3d^2 4p(^2P^o)$	3.2536			

utors. Some important features of photoionization cross sections related to recombination are illustrated in Figure 1. The ground state, $3d^4(^5D)$, which is an equivalent electron state is the most dominant contributor among the quintets of Fe v because of its enhanced background cross sections (Fig. 1*a*). Similar is the case with the equivalent electron state $3d^4(^3H)$, which does not show large number of resonances in Figure 1*b*, yet has comparatively large backgound cross sections that decay slowly with energies and hence contributes to the recombination over a wide range of temperatures. The excited state, $3d^34p(^5G^o)$, dominates recombination at high temperatures because of its extensive resonance structures in σ_{PI}, which have raised the background cross sections in the high energy region (Fig. 1*c*).

Another form of resonances in the σ_{PI} of highly excited states that is important at higher temperature recombinations is known as the PEC (photoexcitation of core) resonances (Yu Yan & Seaton 1987). A PEC resonance is introduced by photoexcitation of the core from the ground state via a dipole allowed transition, while the outer electron remains a spectator. A PEC resonance is more prominent than the narrow Rydberg resonances and can enhance the background considerably. Figure 1*d* illustrates PEC resonances in σ_{PI} of the highly excited state, $3d^38s(^5F)$, where the PEC positions are indicated by arrows. From Table 1 we find that there are four possible PECs, $3d^4(^4F) \rightarrow 3d^24p(^4G^o, {}^4F^o, z\,{}^4D^o, y\,{}^4D^o)$. However, the excited states, $^4G^o$, $^4F^o$, are narrowly spaced, and hence, only three arrows are distinct in the figure.

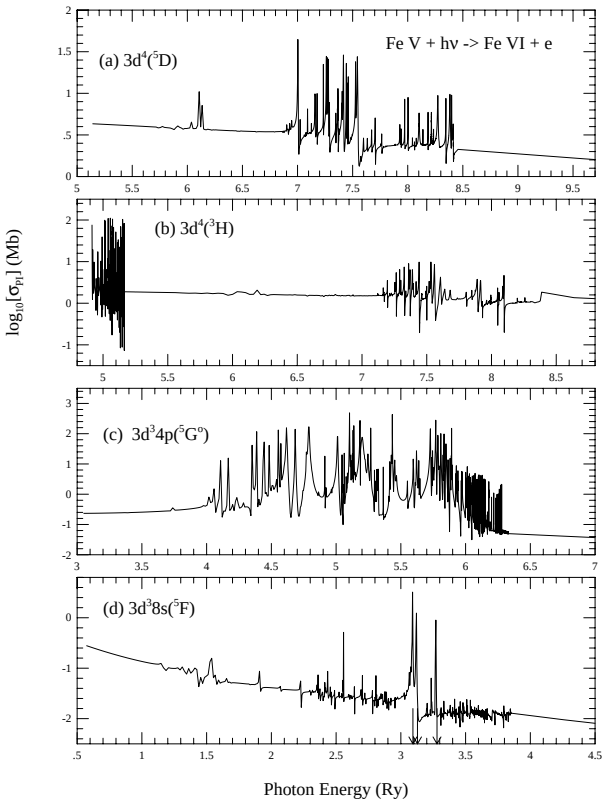

FIG. 1.—Partial photoionization cross sections, σ_{PI}, of the (*a*) ground state, $3d^4\ {}^5D$; (*b*) metastable state, $3d^4\ {}^3H$; (*c*) excited state, $3d^34p\ {}^5G^o$; and (*d*) highly excited state, $3d^3\ {}^4F8s\ {}^5F$, of Fe v leaving the core in the ground state $3d^3\ {}^4F$. Arrows in (*d*) point the PEC positions at $3d^24p(^4G^o, {}^4F^o, z\,{}^4D^o, y\,{}^4D^o)$.

2.2. *High-n States: Collision Strengths for Dielectronic Recombination*

The high-n states, $n_{max} < n \leq \infty$, of group B belong to small energy regions below the thresholds of the target, dominated by dielectronic recombinations (DR) because of weak interaction of the outer electron with the core, which decays through emission of a photon. As the energy approaches the excited threshold, the autoionization rate decreases as ν^{-3}, while the radiative decay increases as ν^3; ν is the effective quantum number of the Rydberg series belonging to the converging threshold. The ab initio theory of DR by Bell & Seaton (1985), as extended in Nahar & Pradhan (1994), is implemented for these states to obtain the DR collision strengths, Ω(DR). The DR rates are obtained through Maxwellian average over Ω(DR).

Calculations are carried out in the close coupling approximation for Ω(DR) using the same wavefunction expansion of 34 states used for σ_{PI}. Present calculations are concerned with channels damping to the target ground state $3d^3\ {}^4F$ only. The core decays radiatively to the ground state via dipole allowed transitions $3d^24p(^4G^o, {}^4F^o, z\,{}^4D^o, y\,{}^4D^o) \rightarrow 3d^4(^4F)$. The radiative transitions probabilities (A-values) for these transitions are taken from the OP work (available through the OP database, TOPbase; Cunto et al. 1993) and are given in Table 2. The computations of Ω(DR) are carried out using the extended code STGFDR (Nahar & Pradhan 1994).

We obtain both forms of Ω(DR), detailed with resonances and the resonance averaged ones. The resonances correspond to the Rydberg series of states $S_t L_t \pi_t vl$ belonging to the converging target threshold $S_t L_t \pi_t$. The features of Ω(DR) are shown in Figure 2, where the dotted curve corresponds to the detailed form and the solid curve to the resonance averaged ones. As ν increases, the resonances become denser while the background rises. Ω(DR) peaks sharply as the energy approaches the converging threshold when the outer electron remains loosely bound in a highly excited state and the core damps radiatively. Ω(DR) converges to the threshold (marked by arrows in Fig. 2) beyond which DR goes to zero as the trapped electron flux in the closed channels below the threshold is released through excitation of the target. Ω(DR) is almost zero at the starting energy $\nu = 10.0$, as seen in the figure, indicating negligible radiation damping below this energy. For the total recombination rate coefficients presented here, we choose the resonance averaged Ω(DR), rather than the detailed one, because of better numerical accuracy.

Independent close coupling calculations for (e, Fe VI) scattering are also carried out for electron impact excitation

TABLE 2

TRANSITION PROBABILITIES

Transition	A_{ji}(a.u.)	$\langle\Omega(\mathrm{DR})\rangle$	$\Omega(\mathrm{EIE})_0$	$\Omega(\mathrm{EIE})_1$
$a\ {}^4F^e \rightarrow z\ {}^4G^o$	2.86(−8)	↓	3.99	3.99
$a\ {}^4F^e \rightarrow z\ {}^4F^o$	2.59(−7)	10.9	5.52	5.52
			Sum = 9.51	9.51
$a\ {}^4F^e \rightarrow z\ {}^4D^o$	2.42(−7)	3.06	2.81	2.88
$a\ {}^4F^e \rightarrow y\ {}^4D^o$	8.78(−8)	1.05	1.04	1.04

NOTE.—Transition probabilities, A_{ji}, for the dipole allowed transitions of the target Fe vi ground state, ^4F, and the peak values of collision strengths for DR, $\langle\Omega(\mathrm{DR})\rangle$, electron-impact excitation collision strengths, $\Omega(\mathrm{EIE})_0$ (excluding contributions of multipole potentials), $\Omega(\mathrm{EIE})_1$ (including these contributions), at these thresholds

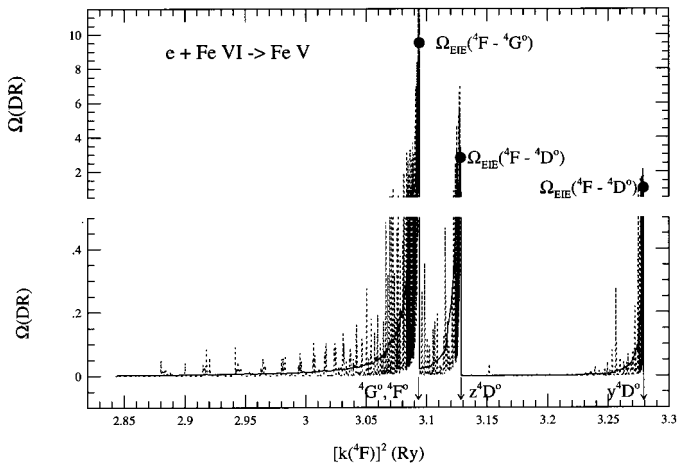

FIG. 2.—DR collision strength, Ω(DR), for the recombination of e + Fe VI → Fe V: detailed with resonances (*dotted curves*) and resonance averaged (*solid curves*). The arrows point the energy positions of the target thresholds $3d^24p(^4G^o, ^4F^o, z\,^4D^o, y\,^4D^o)$, where DR resonances are converging. The filled circles are the excitation collision strength, Ω(EIE), at these thresholds.

(EIE) collision strengths, Ω(EIE), at the target thresholds for a few checks on the recombination calculations. The same eigenfunction expansion of 34 states is used for the calculations and Ω(EIE) is obtained excluding the contributions from multipole potentials in the R-matrix calculations and including them. The comparison between the two values of Ω(EIE) provides an important check for the significance of the higher order multipole potential contributions (Nahar & Pradhan 1994). The present theory of DR collision strengths, based on multichannel quantum defect theory, neglects these contributions. Proper choice of R-matrix boundary and size of R-matrix basis set can compensate the difference introduced by these potentials. Values of Ω(EIE) excluding the contributions (0) and including them (1) are presented in Table 2. Good agreement between the two sets of values indicates insignificant loss of accuracy from multipole potential contributions and that the R-matrix basis set has converged. The values of Ω(EIE) also provides the check of conservation of total electron-photon flux such that the trapped electron flux due to resonances below a threshold equals to that released due to excitation at the threshold. In other words, at an excited threshold the value of $\langle\Omega(\mathrm{DR})\rangle$ should equal to that of Ω(EIE) (without the multipole potentials). Comparison of Ω(EIE) and avaeraged Ω(DR) at the thresholds is made in Table 2. The sum of Ω(EIE) for the first two transitions should be compared with the averaged Ω(DR) peak since the thresholds, $3d^24p(^4G^o, ^4F^o)$, are almost at the same energy (see Table 1). The sum 9.5 of Ω(EIE) is comparable to the Ω(DR) peak of 10.89. The difference can be explained in terms of resolution of the collision strengths with finer mesh and existence of a resonance in Ω(EIE) near the threshold. Good agreement between $\langle\Omega(\mathrm{DR})\rangle$ and Ω(EIE) is seen at other thresholds.

The nonresonant background contributions from the high-n group B states to the total recombination is also included through a "top-up" scheme as explained in Nahar (1996). Although this contribution is negligible at high energies and temperatures, it is considerable for low electron energies at low temperatures.

The complete computation for the total electron-ion recombination has required a maximum memory size of 24 Mwords for about 100 channels and over 320 CPU hours on the Cray Y-MP/8E.

3. RESULTS AND DISCUSSIONS

We present the total $\alpha_R(T)$ and state-specific recombination rate coefficients of 1054 bound states of Fe V. The new rates are used to compute ionization fractions in planetary nebulae, under photoionization equilibirum, to demonstrate the differences using currently available rates.

The first 20 state-specific rates of most contributing states of group A, from both the quintet and the triplet symmetries, are listed at four temperatures, 1000, 10,000, 20,000, and 50,000 K in Table 3. They are listed according to their order of contributions to the total $\alpha_R(T)$ at these temperatures. Both the order and the amount of contributions of the states vary with temperature due to the positions and resonance structures in the photoionization cross sections for these states. The individual state recombination rates of the bound states are of importance in the determination of level population, line intensities. It may be noted the rates in the table are the total individual state recombination rate coefficients at the specified temperatures, not the "effective" recombination rate coefficients since no cascade from very high-n states is included.

The total electron-ion recombination rate coefficients, $\alpha_R(T)$, for the recombining ion at ground state are presented in Table 4 for a wide range of temperature, $1. \le \log_{10} T \le 7$, with temperature mesh of $\Delta \log_{10} T = 0.1$ for easy interpolation of the rates. The features of $\alpha_R(T)$ shown in Figure 3 (*solid curve*). The electron-ion recombination starts high at very low temperature mainly through nonresonant recombination, decreases with temperature to a minimum before rising to a high temperature bump at about $\log_{10} T = 5.3$ K when the resonant recombination becomes dominant. After this $\alpha_R(T)$ falls smoothly. In addition to the prominent high-temperature resonant (DR) bump, $\alpha_R(T)$ often exhibits a slight low-temperature bump owing to the low-energy autoionizing resonances near threshold in the cross sections. Such a low-T bump is not seen in $\alpha_R(T)$ for Fe V, although it exists for other iron ions.

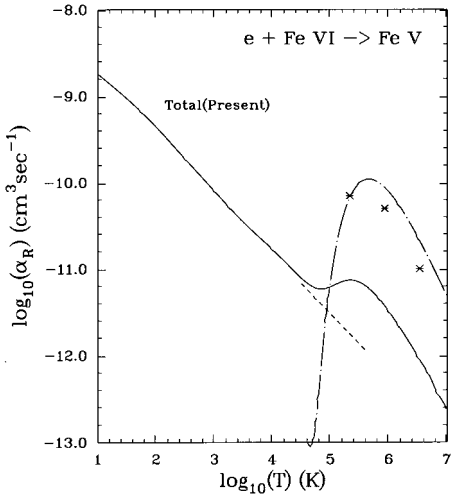

FIG. 3.—Total electron-ion recombination rate coefficients, $\alpha_R(T)$, (*solid curve*) for Fe V of the present work. The dashed curve represents the RR rates, chain-dashed curve represents the DR rates by Woods et al. (1981), and the asterisks refer to DR rates by Hahn (1989).

TABLE 3

INDIVIDUAL STATE RECOMBINATION RATE COEFFICIENTS

1000 K			10,000 K			20,000 K			50,000 K		
State		α_R	State		α_R	State		α_R	State		α_R
$3d^4$	$^5D^e$	4.20E−12	$3d^4$	$^5D^e$	1.35E−12	$3d^4$	$^5D^e$	9.68E−13	$3d^4$	$^5D^e$	6.42E−13
$3d^3\,^4F^e\,4f$.....	$^5I^o$	2.77E−13	$3d^3\,^4F^e\,4f$	$^5I^o$	8.37E−14	$3d^3\,^4F^e\,4f$	$^5I^o$	5.67E−14	$3d^3\,^4F^e\,4s$	$^5F^e$	2.57E−13
$3d^3\,^4F^e\,5f$.....	$^5I^o$	2.27E−13	$3d^3\,^4F^e\,5f$	$^5I^o$	6.90E−14	$3d^3\,^4F^e\,4d$.....	$^5H^e$	5.17E−14	$3d^3\,^4F^e\,4p$	$^5G^o$	8.48E−14
$3d^3\,^4F^e\,4f$.....	$^5H^o$	2.23E−13	$3d^3\,^4F^e\,4d$.....	$^5H^e$	6.77E−14	$3d^3\,^4F^e\,4s$	$^5F^e$	5.17E−14	$3d^3\,^4F^e\,4d$	$^5G^e$	5.23E−14
$3d^3\,^4F^e\,4d$	$^5H^e$	2.04E−13	$3d^3\,^4F^e\,4f$	$^5H^o$	6.72E−14	$3d^3\,^4F^e\,5f$	$^5I^o$	4.68E−14	$3d^3\,^4P^e\,4s$	$^5P^e$	5.23E−14
$3d^3\,^4F^e\,5f$.....	$^5H^o$	1.86E−13	$3d^3\,^4F^e\,5f$	$^5H^o$	5.64E−14	$3d^3\,^4F^e\,4d$.....	$^5G^e$	4.64E−14	$3d^3\,^4F^e\,4d$	$^5H^e$	5.20E−14
$3d^3\,^4F^e\,4f$.....	$^5G^o$	1.80E−13	$3d^3\,^4F^e\,4d$.....	$^5G^e$	5.61E−14	$3d^3\,^4F^e\,4f$	$^5H^o$	4.54E−14	$3d^3\,^4F^e\,4f$.....	$^5I^o$	4.52E−14
$3d^3\,^4F^e\,4d$	$^5G^e$	1.68E−13	$3d^3\,^4F^e\,4f$	$^5G^o$	5.43E−14	$3d^3\,^4F^e\,5f$	$^5H^o$	3.82E−14	$3d^3\,^4F^e\,4p$	$^5F^o$	4.24E−14
$3d^3\,^4F^e\,6f$.....	$^5I^o$	1.57E−13	$3d^3\,^4F^e\,4p$.....	$^5G^o$	4.79E−14	$3d^3\,^4F^e\,4f$	$^5G^o$	3.66E−14	$3d^3\,^4F^e\,5d$	$^5H^e$	3.89E−14
$3d^3\,^4F^e\,5f$.....	$^5G^o$	1.52E−13	$3d^3\,^4F^e\,6f$	$^5I^o$	4.78E−14	$3d^3\,^4F^e\,4p$.....	$^5G^o$	3.62E−14	$3d^3\,^4F^e\,4d$	$^5F^e$	3.56E−14
$3d^3\,^4F^e\,4p$	$^5G^o$	1.45E−13	$3d^3\,^4F^e\,5f$	$^5G^o$	4.59E−14	$3d^3\,^4F^e\,6f$	$^5I^o$	3.25E−14	$3d^3\,^4F^e\,4f$.....	$^5H^o$	3.21E−14
$3d^3\,^4F^e\,6f$.....	$^5H^o$	1.29E−13	$3d^3\,^4F^e\,4s$	$^5F^e$	4.04E−14	$3d^3\,^4F^e\,4d$.....	$^5F^e$	3.12E−14	$3d^3\,^4F^e\,4d$	$^5D^e$	2.75E−14
$3d^3\,^4F^e\,4s$	$^5F^e$	1.20E−13	$3d^3\,^4F^e\,4d$.....	$^5F^e$	3.96E−14	$3d^3\,^4F^e\,5f$	$^5G^o$	3.11E−14	$3d^3\,^4P^e\,4d$	$^5D^e$	2.71E−14
$3d^3\,^4F^e\,4f$.....	$^5F^o$	1.20E−13	$3d^3\,^4F^e\,6f$	$^5H^o$	3.93E−14	$3d^3\,^4F^e\,6f$	$^5H^o$	2.67E−14	$3d^3\,^4F^e\,5f$.....	$^5I^o$	2.70E−14
$3d^3\,^4F^e\,4d$	$^5F^e$	1.19E−13	$3d^3\,^4F^e\,4f$	$^5F^o$	3.60E−14	$3d^3\,^4F^e\,4p$.....	$^5F^o$	2.58E−14	$3d^3\,^4F^e\,4f$.....	$^5G^o$	2.49E−14
$3d^3\,^4F^e\,7f$.....	$^5I^o$	1.08E−13	$3d^3\,^4F^e\,4p$.....	$^5F^o$	3.43E−14	$3d^3\,^4F^e\,4f$	$^5F^o$	2.41E−14	$3d^3\,^4F^e\,4p$	$^5D^o$	2.46E−14
$3d^3\,^4F^e\,6f$.....	$^5G^o$	1.05E−13	$3d^3\,^4F^e\,7f$	$^5I^o$	3.31E−14	$3d^3\,^4F^e\,4d$.....	$^5D^e$	2.37E−14	$3d^3\,^4F^e\,5f$.....	$^5H^o$	2.26E−14
$3d^3\,^4F^e\,5f$.....	$^5F^o$	1.05E−13	$3d^3\,^4F^e\,6f$	$^5G^o$	3.20E−14	$3d^3\,^4F^e\,7f$	$^5I^o$	2.26E−14	$3d^3\,^4F^e\,6f$.....	$^5I^o$	1.86E−14
$3d^3\,^4F^e\,4p$	$^5F^o$	1.04E−13	$3d^3\,^4F^e\,5f$	$^5F^o$	3.16E−14	$3d^3\,^4F^e\,6f$	$^5G^o$	2.18E−14	$3d^3\,^4F^e\,5f$.....	$^5G^o$	1.80E−14
$3d^3\,^4F^e\,4d$	$^5D^e$	9.37E−14	$3d^3\,^4F^e\,4d$.....	$^5D^e$	3.08E−14	$3d^3\,^4F^e\,5f$	$^5F^o$	2.12E−14	$3d^3\,^4F^e\,4f$.....	$^5F^o$	1.69E−14
Sum		7.13E−12			2.26E−12			1.64E−12			1.54E−12
Total		7.92E−11			1.67E−11			1.05E−11			6.20E−12
% Contribution		9%			14%			16%			25%
$3d^4$	$^3H^e$	1.68E−11	$3d^4$	$^3H^e$	1.84E−12	$3d^4$	$^3H^e$	1.15E−12	$3d^4$	$^3H^e$	5.88E−13
$3d^4$	$^3G^e$	4.31E−12	$3d^4$	$^3G^e$	1.27E−12	$3d^4$	$^3G^e$	8.38E−13	$3d^4$	$^3G^e$	4.44E−13
$3d^4$	$^3F^e$	2.11E−12	$3d^4$	$^3F^e$	7.03E−13	$3d^4$	$^3F^e$	4.74E−13	$3d^4$	$^3F^e$	2.42E−13
$3d^4$	$^3F^e$	1.37E−12	$3d^4$	$^3F^e$	4.09E−13	$3d^4$	$^3F^e$	3.08E−13	$3d^4$	$^3F^e$	1.60E−13
$3d^4$	$^3P^e$	8.48E−13	$3d^4$	$^3P^e$	4.04E−13	$3d^4$	$^3P^e$	2.66E−13	$3d^4$	$^3P^e$	1.41E−13
$3d^4$	$^3D^e$	6.24E−13	$3d^4$	$^3D^e$	2.25E−13	$3d^4$	$^3D^e$	1.62E−13	$3d^4$	$^3D^e$	8.54E−14
$3d^3\,^2H^e\,4d$.....	$^3H^e$	3.92E−13	$3d^3\,^2F^e\,4p$.....	$^3G^o$	1.10E−13	$3d^3\,^2F^e\,4p$.....	$^3G^o$	7.25E−14	$3d^3\,^4F^e\,4s$	$^3F^e$	4.59E−14
$3d^3\,^2H^e\,7h$.....	$^3F^o$	3.21E−13	$3d^3\,^2F^e\,4p$.....	$^3F^o$	9.32E−14	$3d^3\,^2F^e\,4p$.....	$^3F^o$	6.12E−14	$3d^3\,^2H^e\,4s$	$^3H^e$	4.08E−14
$3d^3\,^2H^e\,6h$.....	$^3F^o$	2.29E−13	$3d^4$	$^3P^e$	8.24E−14	$3d^4$	$^3P^e$	4.79E−14	$3d^3\,^2F^e\,4p$	$^3G^o$	2.81E−14
$3d^3\,^2H^e\,6h$.....	$^3D^o$	2.07E−13	$3d^3\,^2F^e\,5p$.....	$^3G^o$	6.59E−14	$3d^3\,^2F^e\,5p$.....	$^3G^o$	4.32E−14	$3d^3\,^4F^e\,4d$	$^3H^e$	2.49E−14
$3d^3\,^2G^e\,4d$	$^3H^e$	1.38E−13	$3d^3\,^2F^e\,5p$.....	$^2f^o$	5.55E−14	$3d^3\,^2F^e\,5p$.....	$^2f^o$	3.64E−14	$3d^3\,^2F^e\,4p$	$^2f^o$	2.34E−14
$3d^4$	$^3P^e$	1.33E−13	$3d^3\,^2F^e\,4p$.....	$^3D^o$	5.50E−14	$3d^3\,^2F^e\,4p$.....	$^3D^o$	3.61E−14	$3d^3\,^4F^e\,4d$	$^3G^e$	2.33E−14
$3d^3\,^4F^e\,4f$.....	$^3I^o$	1.31E−13	$3d^3\,^2F^e\,6p$.....	$^3G^o$	4.32E−14	$3d^3\,^4F^e\,4d$.....	$^3H^e$	2.85E−14	$3d^3\,^2G^e\,4s$	$^3G^e$	2.11E−14
$3d^3\,^4F^e\,5f$.....	$^3I^o$	1.13E−13	$3d^3\,^4F^e\,4f$	$^3I^o$	3.96E−14	$3d^3\,^2F^e\,6p$.....	$^3G^o$	2.84E−14	$3d^3\,^4F^e\,4d$	$^3F^e$	1.94E−14
$3d^3\,^4F^e\,4f$.....	$^3H^o$	1.08E−13	$3d^3\,^4F^e\,4d$.....	$^3H^e$	3.77E−14	$3d^3\,^4F^e\,4f$	$^3I^o$	2.66E−14	$3d^3\,^2H^e\,4d$.....	$^3K^e$	1.86E−14
$3d^3\,^2H^e\,4d$.....	$^3K^e$	9.76E−14	$3d^3\,^2F^e\,6p$.....	$^2f^o$	3.65E−14	$3d^3\,^4F^e\,4s$	$^3F^e$	2.53E−14	$3d^4$	$^3P^e$	1.86E−14
$3d^3\,^4F^e\,4d$	$^3H^e$	9.56E−14	$3d^3\,^2F^e\,5p$.....	$^3D^o$	3.50E−14	$3d^3\,^2F^e\,6p$.....	$^2f^o$	2.39E−14	$3d^3\,^2F^e\,5p$	$^3G^o$	1.62E−14
$3d^3\,^4F^e\,5f$.....	$^3H^o$	9.46E−14	$3d^3\,^4F^e\,5f$	$^3I^o$	3.40E−14	$3d^3\,^4F^e\,4d$.....	$^3G^e$	2.35E−14	$3d^3\,^4F^e\,4p$	$^3G^o$	1.60E−14
$3d^3\,^2H^e\,4d$.....	$^3I^e$	8.90E−14	$3d^3\,^4F^e\,4f$	$^3H^o$	3.30E−14	$3d^3\,^2F^e\,5p$.....	$^3D^o$	2.29E−14	$3d^3\,^4F^e\,4f$.....	$^3I^o$	1.49E−14
$3d^3\,^4F^e\,4d$	$^3G^e$	8.84E−14	$3d^3\,^4F^e\,4d$.....	$^3G^e$	3.07E−14	$3d^3\,^4F^e\,5f$	$^3I^o$	2.29E−14	$3d^3\,^2F^e\,4p$	$^3D^o$	1.37E−14
Sum		2.84E−11			5.60E−12			3.70E−12			1.98E−12
Total		7.92E−11			1.67E−11			1.05E−11			6.20E−12
% Contribution		36.%			34.%			35.%			32.%

NOTES.—Individual state recombination rate coefficients (in units of $cm^3\ s^{-1}$) for e + Fe VI→Fe V at four temperature, T = 1000, 10,000, 20,000, and 50,000 K. The first 20 dominant quintets and tiplets are listed in order of their contributions. Their sum percentage is specified below.

Previous calculations of recombination to Fe V were carried out by Woods et al. (1981) and Hahn (1989) using simpler approximations. Woods et al. obtained the RR rate coefficients (Fig. 3, *dashed curve*), valid over a smaller range of temperatures, from σ_{PI} calculated in the central field and the hydrogenic approximations that do not consider any autoionizing resonances. They obtained the DR rate coefficients (*dot-dashed curve*) using the Burgess general formula (Burgess 1965). The oscillator strengths used in the Burgess formula were unreliable and incomplete as stated by the authors. Hahn introduced an empirical formula based on the Burgess general formula for DR rates for recombination to Fe V (Fig. 3, *asterisks*). However, he also expressed uncertainty in the rates because of unavailability of accurate atomic data. Comparison of $\alpha_R(T)$ in the temperature region, $4.5 \le \log_{10}(T) \le 4.9$, shows that the sum of RR and DR for the total by Woods et al., although lower, are close to the present values. The reason is, as we find in the present computations, that the contributions from the nonresonant background cross sections of high-n states, $n_{max} < n \le \infty$, dominate the recombination at low temperatures, and continue to do so even beyond 10^5 K. However, considerable difference is found between the rates of present and of Burgess formula used by Woods et al., and Hahn. In addi-

TABLE 4

TOTAL RECOMBINATION RATE COEFFICIENTS

$\log_{10} T$	α_R	$\log_{10} T$	α_R	$\log_{10} T$	α_R
1.0.....	1.80E−09	3.1.....	6.67E−11	5.2.....	7.09E−12
1.1.....	1.58E−09	3.2.....	5.62E−11	5.3.....	7.36E−12
1.2.....	1.39E−09	3.3.....	4.75E−11	5.4.....	7.34E−12
1.3.....	1.22E−09	3.4.....	4.03E−11	5.5.....	6.96E−12
1.4.....	1.07E−09	3.5.....	3.44E−11	5.6.....	6.36E−12
1.5.....	9.34E−10	3.6.....	2.95E−11	5.7.....	5.57E−12
1.6.....	8.12E−10	3.7.....	2.56E−11	5.8.....	4.76E−12
1.7.....	7.03E−10	3.8.....	2.22E−11	5.9.....	3.97E−12
1.8.....	6.05E−10	3.9.....	1.93E−11	6.0.....	3.21E−12
1.9.....	5.18E−10	4.0.....	1.67E−11	6.1.....	2.56E−12
2.0.....	4.40E−10	4.1.....	1.44E−11	6.2.....	2.04E−12
2.1.....	3.72E−10	4.2.....	1.23E−11	6.3.....	1.59E−12
2.2.....	3.13E−10	4.3.....	1.05E−11	6.4.....	1.24E−12
2.3.....	2.63E−10	4.4.....	8.99E−12	6.5.....	9.62E−13
2.4.....	2.21E−10	4.5.....	7.75E−12	6.6.....	7.48E−13
2.5.....	1.86E−10	4.6.....	6.81E−12	6.7.....	5.81E−13
2.6.....	1.57E−10	4.7.....	6.19E−12	6.8.....	4.06E−13
2.7.....	1.32E−10	4.8.....	5.88E−12	6.9.....	3.12E−13
2.8.....	1.12E−10	4.9.....	5.89E−12	7.0.....	2.39E−13
2.9.....	9.40E−11	5.0.....	6.18E−12		
3.0.....	7.92E−11	5.1.....	6.63E−12		

NOTES.—Total recombination rate coefficients, $\alpha_R(T)$, in units of cm^3 s^{-1}, for the recombination of e + Fe VI → Fe V. The temperature is given in K.

tion to the stated uncertainties in the oscillator strengths used in the previous works, the difference arises from the overestimation of Burgess formula for ions with strong coupling interactions (Nahar 1996). The formula does not include (1) the interference effect of the resonant DR and continuum background and (2) the autoionization in to the lower states other than the ground state, an important process first pointed out by Jacobs et al. (1977). This latter process reduces DR, considerably if the couplings are strong, as in the present case for Fe V.

The accuracy of the present values of total recombination rate coefficients, $\alpha_R(T)$, may be estmated to be 20%–30% in the temperature range going up to about 6. × 10^5 K corresponding to energy, 3.7225 ryd, of the highest target state $3d^2 4p\ ^2P^o$ in the CC expansion of Fe V (Table 1). The estimation of accuracy of the present results is based on the agreement of calculated energies with the observed ones, use of observed target energies for accurate resonance positions, the general accuracy of the CC method for photoionization cross sections, electron scattering and DR collision strengths, and comparison of the unified method with experiment (Zhang, Nahar, & Pradhan 1998). Beyond the highest target state the cross sections are extrapolated, which may introdue larger uncertainty at higher temperatures. The estimated accuracy for the state-specific rates at higher temperature may have higher uncertainty since the mesh for the high energy resonances is coarser than that in the low-energy region. Inclusion of the relativistic effects could have improved the results but are not expected to be significant since the work on electron-ion scattering for Fe II, III, and IV show relativistic effects to be small (Zhang & Pradhan 1995, 1997). The contributions from highly excited states, beyond the highest target state $^2P^o$ at 3.7225 ryd, are also not expected to be large because of decreasing DR collision strengths, weaker PEC resonances, and exponential decay of Maxwellian distribution function in the rate integral with increasing energy. The other effect, the second-order radiation damping of low-n autoionizing states (below $\nu = 10.$), is not included in the present calculations. The effect is not important for Fe V since the radiative transition rates are of the order of 10^9 or 10^{10} s^{-1} (when the A-values in Table 2 are converted to time unit) and are orders of magnitude lower than typical autoionization rate of 10^{14} s^{-1}.

4. Fe IONIZATION BALANCE IN PLANETARY NEBULAE

In this section we investigate the effects of the new atomic data, photoionization cross sections, and recombination rate coefficients, on the ionization structure of iron. We illustrate this effect for the case of planetary nebulae (PNe), which often show all the ionization stages of iron from Fe II through VII in their optical/UV spectra (e.g., Aller & Keyes 1987; Hyung & Aller 1997). Similar investigation for Fe I–Fe IV was presented for the Orion H II region in Bautista & Pradhan (1998).

In photoionization equilibrium the ionic structure of an element X in the ionization stage X^{i+} is given by

$$N(X^{i+})(\Gamma_i + N_e\,\alpha_i) = N(X^{(i+1)+})\Gamma_{i+1} + N(X^{(i-1)+})N_e\,\alpha_{i-1}, \quad (4)$$

where N_e is the electron density, and α is the recombination coefficient, and Γ is the photoionization rate,

$$\Gamma(s^{-1}) = 4\pi \int_{E_o}^{E_{\max}} F(E)\sigma_E\, dE\ , \quad (5)$$

where σ_E is the total ground state photoionization cross section in cm^2, $F(E)$ is the photoionizing radiation field, and E_o is the ionization potential of X^{i+}.

We study a typical photoionization model of PNe with a $T_{\rm eff}$ = 100,000 K blackbody as ionizing source, an inner radius of 10^{10} cm, and a particle density of 3600 cm^{-3}. We use the computer code CLOUDY (Ferland 1993) for photoionization modeling but incorporate the new atomic for

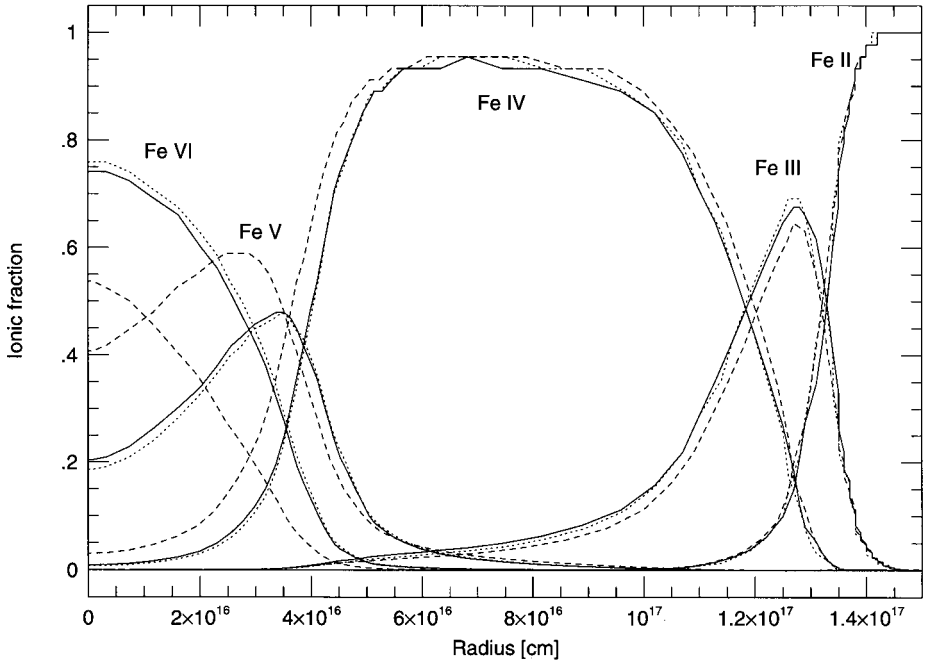

FIG. 4.—Computed ionization structure of iron in a typical planetary nebula. Solid curves are present ion fractions using the new photoionization-recombination data, the dotted curves are those using the new photoionization and recombination rates of Woods et al. (1981) and the dashed curves are those using the available data of Verner et al. (1993) and Woods et al.

Fe I–Fe V, including photoionization cross sections and recombination rate coefficients (see also Bautista & Pradhan 1998 and references therein). The photoionization cross sections used here are Gaussian averaged over resonances as described in Bautista, Romano, & Pradhan (1998). These averaged cross sections are practically much more convenient than detailed cross sections and there is no significant loss of accuracy.

Figure 4 shows the ionization structure of iron (Fe II–Fe VI) in the nebula as calculated using the new cross sections and recombination rates (*solid curves*), new cross sections and recombination rates by Woods et al. (1981) (*dotted curves*), and fitted cross sections by Verner et al. (1993) and the recombination rates by Woods et al. (*dashed curves*). The overall fraction of Fe I is negligible in this case and hence is not presented. The dotted curves follow closely the solid curves, while considerable differences are noted with the dashed curves using earlier data. This indicates that the main differences come from the resonance structures in the photoionization cross sections. The new data result in a reduction of the Fe V fraction of a factor of 2 in the region near illuminated phase of the cloud with respect to previous predictions, while the fraction of Fe VI is increased by almost 40%. The ionic fraction of Fe I–IV are also affected.

Table 5 presents the ionic fractions of Fe I–VI averaged over the whole volume of the nebula. It is shown that the averaged fraction of Fe V decreases by approximately 30%, while the fraction of Fe VI is almost doubled. Further, previous data predicted that the fraction of Fe VI should be about half the fraction of Fe V, but the new data indicate that Fe VI should actually be ~ 1.3 times more abundant than Fe V. Most of the change in the ionization structure is due to the structure of the new photoionization cross sections, in particular the large near-threshold resonance in the total photoionization cross sections of the ^5D ground state of Fe V (see Fig. 2 of Bautista 1996). Nevertheless, it is always essential to try to preserve the consistency between photoionization and recombination rates.

The change observed in the ionization structure of iron is expected to have an important effect on Fe abundance estimations in PNe. This is because Fe IV is the dominant ionization stage in the plasma but in most cases, except when very high electron densities are present (Bautista & Pradhan 1998), emission lines from this ion are too weak to be detected. Then, abundance estimations must rely entirely on observations of Fe V and Fe VI to estimate ionic corrections that account for the majority of Fe that is unseen.

5. CONCLUSION

The total and state-specific electron-ion recombination rate coefficients are obtained for the recombined ion Fe V in the close coupling approximation employing a unified treatment. To our knowledge, no detailed study for the election-ion recombination for Fe V was carried out prior to this work. Currently used rates for Fe V (not available below $\log_{10}(T) = 4.5$ K) were obtained using simple approximations and unreliable atomic data. Present rates differ

TABLE 5

AVERAGED IONIC FRACTIONS OF IRON IN A MODEL PN AT $T_{\rm eff} = 10^5$ K

Calculation	Fe I	Fe II	Fe III	Fe IV	Fe V	Fe VI
Earlier $\sigma_{\rm PI}$, α_R	3.3×10^{-4}	0.166	0.109	0.495	0.145	0.080
New $\sigma_{\rm PI}$, α_R	1.5×10^{-4}	0.145	0.127	0.470	0.112	0.140

considerably from those, particularly in the higher temperature region, above $\log_{10}(T) = 4.9$ K. The present total rates should be accurate to 20%–30% for most of the temperature region of Fe V abundance in astrophysical sources. These rates, along with the *total* photoionization cross sections obtained with the same close coupling expansion (Bautista 1996), provide self-consistent atomic data for accurate calculations of ionization balance for plasmas in photoionization and coronal equilibria.

Application of the new results on medium excitation planetary nebulae show that the ionic fraction ratio Fe VI/Fe V changes from 0.5, obtained using earlier results, to 1.3. This indicates that the new photoionization cross sections and recombination rate coefficients for Fe I–Fe V will have a significant effect on the modeling of astrophysical objects.

All data may be obtained from the first author by e-mail at nahar@astronomy.ohio-state.edu.

This work was supported partially by the NSF (AST 98-70089) and the NASA Astrophysics Data Program. We would like to thank Professor Anil K. Pradhan for contributions. The computations were carried out at the Supercomputer Center in Columbus, Ohio.

REFERENCES

Aller, L. H., & Keyes, C. D. 1987, ApJS, 65, 405
Barstow, M. A., Hubeny, I., Lanz, T., Holberg, J. B., & Sion, E. M. 1996, in Astrophysics in the Extreme Ultraviolet, ed. S. Bowyer & R. F. Malina (Dordrecht: Kluwer), 203
Bautista, M. A. 1996, A&AS, 119, 105
Bautista, M. A., & Pradhan, A. K. 1998, APJ, 492, 650
Bautista, M. A., Romano, P., & Pradhan, A. K. 1998, ApJS, 118, 259
Bell, R. H., & Seaton, M. J. 1985, J. Phys. B, 18, 1589
Berrington, K. A., Burke, P. G., Butler, K., Seaton, M. J., Storey, P. J., Taylor, K. T., & Yan, Yu. 1987, J. Phys. B, 20, 6379
Burgess, A. 1965, ApJ, 141, 1588
Cunto, W., Mendoza, C., Ochsenbein, F., & Zeippen, C. J. 1993, A&AS, 275, L5
Eissner, W. 1991, J. Phys. IV (Paris), C1, 3
Eissner, W., Jones, W., & Nussbaumer, N. 1974, Comput. Phys. Commun., 8, 270
Ferland, G. J. 1993, University of Kentucky Department of Physics and Astronomy Int. Rep. (CLOUDY) (Lexington: Univ. Kentucky)
Hahn, Y. 1989, J. Quant. Spectrosc. Radiat. Transfer, 41, 315
Hummer, D. G., Berrington, K. A., Eissner, W., Pradhan, A. K., Saraph, H. E., & Tully, J. A. 1993, A&A, 279, 298
Hyung, S., & Aller, L. H. 1997, ApJ, 491, 242
Jacobs, V. L., Davis, J., Keppler, P. C., & Blaha, M. 1977, ApJ, 215, 690
Koester, D. 1996, in Astrophysics in the Extreme Ultraviolet, ed. S. Bowyer & R. F. Malina (Dordrecht: Kluwer), 185
Nahar, S. N. 1996, Phys. Rev. A, 53, 2417
———. 1997, Phys. Rev. A, 55, 1980
Nahar, S. N., Bautista, M. A., & Pradhan, A. K. 1997, ApJ, 479, 497
———. 1998, Phys. Rev. A, 58, 4593
Nahar, S. N., & Pradhan, A. K. 1994, Phys. Rev. A, 49, 1816
———. 1995, ApJ, 447, 966
Osterbrock, D. E. 1989, in Astrophysics of Gaseous Nebulae and Active Galactic Nuclei (Mill Valley: University Science Books)
Peimbert, M. 1989, in IAU Symp. 131, Planetary Nebulae, ed. S. Torres-Peimbert (Dordrecht: Reidel), 577
Seaton, M. J. 1987, J. Phys. B, 20, 6363
Vennes, S. 1996, in Astrophysics in the Extreme Ultraviolet, ed. S. Bowyer & R. F. Malina (Dordrecht: Kluwer), 193
Verner, D. A., Yakovlev, D. G., Brand,I. M., Trzhaskovskaya, M. B. 1993, At. Data Nucl. Data Tables, 55, 233
Woods, D. T., Shull, J. M., & Sarazin, C. L. 1981, ApJ, 249, 399
Yu Yan, & Seaton, M. J. 1987, J. Phys. B, 20, 6409
Zhang, H. L., Nahar, S. N., & Pradhan, A. K. 1998, submitted
Zhang, H. L., & Pradhan, A. K. 1995, J. Phys.B, 28, 3403
———. 1997, A&AS, 126, 373